Valence isoelectronic substitution in the B8− and B9− molecular wheels by an Al dopant atom: Umbrella-like structures of AlB7− and AlB8−

Timur R. Galeev, Constantin Romanescu, Wei-Li Li, Lai-Sheng Wang, and Alexander I. Boldyrev

Citation: J. Chem. Phys. **135**, 104301 (2011); doi: 10.1063/1.3625959
View online: http://dx.doi.org/10.1063/1.3625959
View Table of Contents: http://jcp.aip.org/resource/1/JCPSA6/v135/i10
Published by the American Institute of Physics.

Valence isoelectronic substitution in the B_8^- and B_9^- molecular wheels by an Al dopant atom: Umbrella-like structures of AlB_7^- and AlB_8^-

Timur R. Galeev,[1] Constantin Romanescu,[2] Wei-Li Li,[2] Lai-Sheng Wang,[2,a)] and Alexander I. Boldyrev[1,b)]
[1]*Department of Chemistry and Biochemistry, Utah State University, 0300 Old Main Hill, Logan, Utah 84322-0300, USA*
[2]*Department of Chemistry, Brown University, Providence, Rhode Island 02912, USA*

(Received 17 June 2011; accepted 27 July 2011; published online 8 September 2011)

The structures and the electronic properties of two aluminum-doped boron clusters, AlB_7^- and AlB_8^-, were investigated using photoelectron spectroscopy and *ab initio* calculations. The photoelectron spectra of AlB_7^- and AlB_8^- are both broad, suggesting significant geometry changes between the ground states of the anions and the neutrals. Unbiased global minimum searches were carried out and the calculated vertical electron detachment energies were used to compare with the experimental data. We found that the Al atom does not simply replace a B atom in the parent B_8^- and B_9^- planar clusters in AlB_7^- and AlB_8^-. Instead, the global minima of the two doped-clusters are of umbrella shapes, featuring an Al atom interacting ionically with a hexagonal and heptagonal pyramidal B_7 (C_{6v}) and B_8 (C_{7v}) fragment, respectively. These unique umbrella-type structures are understood on the basis of the special stability of the quasi-planar B_7^{3-} and planar B_8^{2-} molecular wheels derived from double aromaticity. © *2011 American Institute of Physics*. [doi:10.1063/1.3625959]

I. INTRODUCTION

The eight- and nine-atom anionic clusters of boron form beautiful molecular wheels with a central B atom and a monocyclic B_7 and B_8 ring, respectively.[1] The chemical bonding in these molecular wheels is interesting. The peripheral B_7 and B_8 rings are bonded by classical two-center-two-electron (2c–2e) bonds, whereas the central B atom is bonded with the outer ring via three delocalized σ and three delocalized π bonds. Thus, the negatively charged nine-atom (B_9^-) cluster with 28 valence electrons is closed shell with a perfect D_{8h} symmetry. Among its 28 valence electrons, 16 are used to form 8 classical 2c–2e peripheral bonds, 6 are used to form three delocalized σ bonds, and the remaining 6 electrons form three delocalized π bonds. The delocalized σ and π bonding each conform with the $(4n + 2)$ Hückel rule for aromaticity, giving rise to double aromaticity and high electronic stability for the B_9^- molecular wheel. To fulfill the double aromaticity, the eight-atom cluster requires 26 valence electrons: 14 for the seven classical peripheral 2c–2c B–B bonds, 6 delocalized σ electrons, and 6 delocalized π electrons. Thus, the B_8^{2-} cluster is a closed shell system with a perfect D_{7h} symmetry, whereas the B_8^- cluster with 25 valence electrons possesses a planar C_{2v} structure slightly distorted from the D_{7h} structure due to the Jahn-Teller effect because the highest occupied molecular orbital (HOMO) is a doubly degenerate orbital ($1e_1''$). The neutral B_8 cluster possesses a perfect D_{7h} structure with a half-filled HOMO ($1e_1''^2$) and a triplet ground electronic state ($^3A_2$). In the present article, we address the issue of valence isoelectronic substitution by an Al atom in the B_8 and B_9 molecular wheels. Understanding the structures of the doped clusters, AlB_7^- and AlB_8^-, will provide further insight into the bonding and stability of the planar boron clusters.[2,3]

Despite recent advances in the spectroscopy of boron clusters,[2] relatively little is known about metal-doped boron clusters. There are only two prior joint experimental and theoretical studies characterizing metal-doped boron clusters, namely $Au_2B_7^-$ and AuB_{10}^-.[4,5] It was found that in the global minimum structures gold mimics the behavior of H atoms,[6] i.e., the gold atoms are covalently bonded to the corresponding boron clusters. Mass spectra of $Al_nB_m^-$ clusters have been reported,[7] as well as photoelectron spectra of one or two B atoms doped aluminum clusters.[8] A number of theoretical calculations on Al–B mixed clusters have also been reported.[9–12] Theoretical studies on neutral AlB_9, suggest a D_{9h} global minimum with Al in the center of a B_9 ring.[9,12]

Recently, we reported a joint PES and computational study of two Al doped boron clusters, AlB_6^- and AlB_{11}^-, aimed at investigating the structural effects of valence isoelectronic substitution on two quasi-planar boron clusters: B_7^- ($^3A_1$, C_{6v}) and B_{12}^- ($^2A'$, C_s).[13] We showed that the Al atom replaces a peripheral B atom. Such substitution slightly expands the circumferences of the clusters and induces planarization in AlB_6^- and AlB_{11}^- relative to the quasi-planar parent boron clusters. In the current article, we expand the scope of our initial study and examine the structural changes of the molecular wheels (B_8^- and B_9^-) upon B-atom substitution by Al. We have obtained photoelectron spectra of AlB_7^- and AlB_8^- at two photodetachment laser energies, 6.424 and 4.661 eV. Unbiased global minimum searches were used to find the lowest energy isomers. One should not expect that geometries of the aluminum-doped clusters are the same as

a)Electronic mail: Lai-Sheng_Wang@brown.edu.
b)Electronic mail: a.i.boldyrev@usu.edu.

the global minimum structures of unsubstituted ones. Indeed, in this work, we found that AlB_7^- and AlB_8^- have different geometries compared to B_8^- and B_9^-. We show that in both cases the Al atom is ionically bonded to a quasi-planar boron cluster, C_{6v} B_7 and C_{7v} B_8, respectively, similar to the LiB_8^- cluster reported earlier.[14] We would like to mention two recent comprehensive reviews[15,16] on negative molecular ions where various theoretical techniques and applications were discussed.

II. EXPERIMENTAL METHOD

The experiment was performed using a magnetic-bottle PES apparatus equipped with a laser vaporization cluster source, details of which have been published Refs.17 and 18. Briefly, the aluminum-doped boron clusters were produced by laser vaporization of a disk target made of isotopically enriched ^{10}B (~10wt. %), Al (~2.5wt. %), balanced by Bi. The ^{11}B to ^{10}B ratio is 1:24. The clusters entrained in the helium carrier gas underwent a supersonic expansion to form a collimated molecular beam. The cluster composition and temperature to some degree were controlled by the time delay between the pulsed He carrier gas and the vaporization laser.[19,20] To achieve an even higher degree of vibrational cooling of the clusters some experiments were carried out using a mixture of 5% Ar in He as a carrier gas. The last approach was previously shown to produce cold gold cluster anions via the observation of Ar-tagged gold clusters.[21] The negatively charged clusters were extracted from the cluster beam and analyzed with a time-of-flight mass spectrometer. The clusters of interest were mass-selected and decelerated before being intercepted by the probe photodetachment laser beam: 193 nm (6.424 eV) from an ArF excimer laser and 266 nm (4.661 eV) from an Nd:YAG laser. Photoelectrons were collected at nearly 100% efficiency by a magnetic bottle and analyzed in a 3.5 m long electron flight tube. The photoelectron spectra were calibrated using the known spectra of Bi^-. The kinetic energy resolution of the magnetic bottle apparatus, $\Delta E/E$, was typically better than 2.5%, i.e., ~25 meV for 1 eV electrons.

III. THEORETICAL METHODS

The computational search for the global minima of the AlB_7^- and AlB_8^- clusters was performed using the Coalescence Kick (CK) program written by Averkiev.[22] The CK method subjects large populations of randomly generated structures to a coalescence procedure in which all atoms are pushed gradually to the molecular center of mass to avoid generation of fragmented structures and then optimized to the nearest local minima. The CK calculations were performed using the B3LYP (Refs. 23–25) hybrid method with the small split-valence basis set 3–21G.[26] The low-lying isomers revealed by the search were reoptimized with follow-up frequency calculations at the B3LYP level of theory using the 6–311+G* basis set.[27–30] To avoid high spin contaminations, single point calculations for the lowest energy structures of AlB_7^- (doublet ground state) were performed using the restricted coupled cluster [RCCSD(T)] method[31–33] with the 6–311+G(2*df*) basis set at the B3LYP/6–311+G* optimized geometries. Single-point calculations for the lowest energy structures of AlB_8^- (singlet ground state) were done using the coupled cluster [RCCSD(T)] method with the 6–311+G(2*df*) basis set at the B3LYP/6–311+G* optimized geometries.

The vertical electron detachment energies (VDEs) were calculated using the UCCSD(T)/6–311+G(2*df*) method, the outer valence Green function method[34–37] [R(U)OVGF/6–311+G(2*df*)] and the time-dependent DFT method,[36,37] TD-B3LYP/6–311+G(2*df*),[38,39] and TD-PBE1PBE/6–311+G(2*df*),[40,41] all at the B3LYP/6–311+G* optimized geometries. In the last approach, for AlB_8^-, the first VDE was calculated as the lowest transition from the singlet state of the AlB_8^- anion into the final lowest doublet state of the neutral AlB_8 species at the geometry optimized for the anion. Then, the vertical excitation energies of the neutral species calculated at the anion geometry were added to the first VDE to obtain the second and higher VDEs. For AlB_7^-, the first two VDEs were calculated as the lowest transition from the doublet ground state of the anion into the final lowest singlet and triplet states of the neutral species at the anion geometry at the geometry optimized for the anion. Then, in order to obtain higher VDEs, the vertical excitation energies of the neutral species at the anion geometry calculated for the singlet and triplet states were added to the two lowest VDEs with the singlet and triplet final states, respectively. Core electrons were frozen in treating the electron correlation at the CCSD(T) and OVGF levels of theory.

Chemical bonding analysis was performed using the natural bond orbital (NBO) (Refs. 42–44) analysis. The B3LYP, UCCSD(T), R(U)OVGF, and TD-B3LYP calculations were performed using the GAUSSIAN 03 software[45] and RCCSD(T) calculations were performed using the MOLPRO program.[46] The MOLDEN 3.4 (Ref. 47) and MOLEKEL 5.4.0.8 (Ref. 48) programs were used for molecular structure visualizations.

IV. EXPERIMENTAL RESULTS

The photoelectron spectra of AlB_7^- and AlB_8^- at 266 and 193 nm are shown in Figs. 1 and 2, respectively. The major detachment features are labeled with letters and the measured vertical detachment energies are given in Tables I and II, where they are compared with theoretical calculations at various levels (*vide infra*). Commonly, the peak marked as X represents the transition between the ground electronic states of the anion and the neutral species, while the higher binding energy peaks (A, B…) denote transitions to excited electronic states of the neutral cluster.

A. AlB_7^-

A single broad band is observed in the 266 nm spectrum of AlB_7^- (Fig. 1(a)) with a VDE of 3.3 ± 0.1 eV. There seems to be a shoulder on the higher binding energy side, suggesting that the band may contain multiple electronic transitions.

Under our experimental conditions, the clusters were fairly cold, as shown, recently, in our studies of AlB_6^- and AlB_{11}^-.[13] Thus, the broad PES band observed suggests a large geometry change between the ground states of the AlB_7^- anion and that of AlB_7 neutral. The broad band and

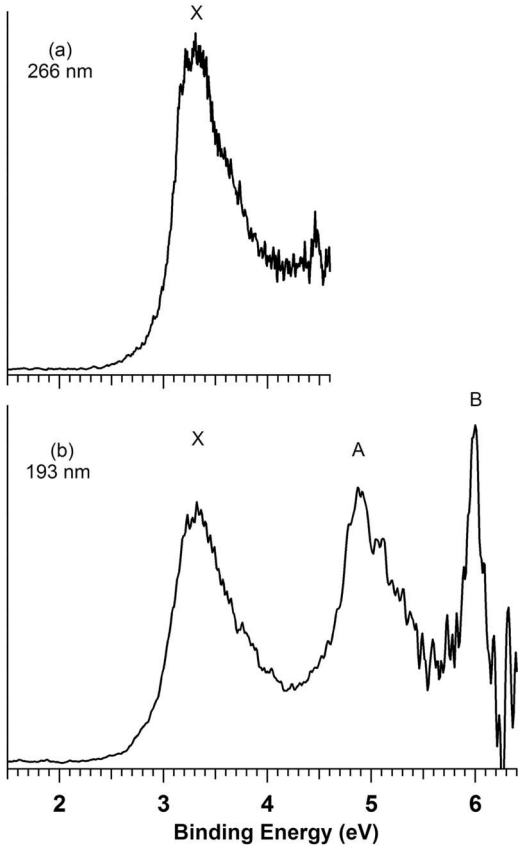

FIG. 1. Photoelectron spectra of AlB_7^- at (a) 266 nm and (b) 193 nm photodetachment wavelengths.

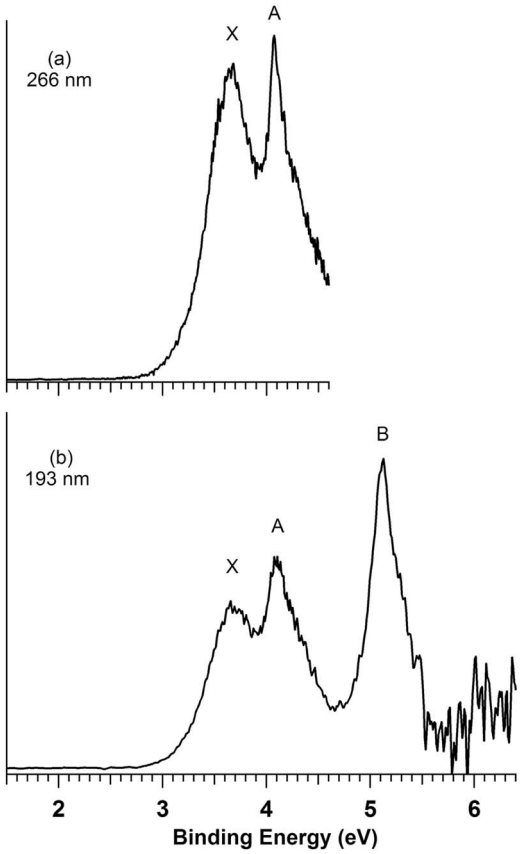

FIG. 2. Photoelectron spectra of AlB_8^- at (a) 266 nm and (b) 193 nm photodetachment wavelengths.

the long tail on the lower binding energy side prevent us from accurately measuring the adiabatic detachment energy. Only a detachment threshold can be estimated to be ~2.8 eV. The 193 nm spectrum reveals two additional strong PES bands, A and B. The A band with a VDE of 4.89 ± 0.06 eV is broad and contains shoulder in both the lower and higher binding energy sides, suggesting that it contains multiply detachment transitions. The weak sharp band at ~4.5 eV in the 266 nm spectrum becomes part of the low binding energy shoulder on the A band. The B band with a VDE of 5.98 ± 0.03 eV is relatively sharp and well defined and it should correspond to a singly electronic transition.

TABLE I. Experimentally observed and theoretically calculated VDEs for the isomer I.1 (C_{6v}, $^2A_1$) of AlB_7^-. All energies are in eV.

Feature	VDE (expt.)[a]	Final state and electronic configuration	VDE (theoretical) TD-B3LYP[b]	TD-PBE1PBE[c]	UOVGF[d]	UCCSD(T)[e]
X	3.3(1)	$^3E_1$, $\{\ldots 3a_1^2 1b_1^2 2e_1^4 3e_1^3 4a_1^1\}$	3.02	3.28	3.30 (0.88)	3.27
		$^1E_1$, $\{\ldots 3a_1^2 1b_1^2 2e_1^4 3e_1^3 4a_1^1\}$	[f]	3.42	[g]	[g]
	4.45(5)	$^1A_1$, $\{\ldots 3a_1^2 1b_1^2 2e_1^4 3e_1^4 4a_1^0\}$	4.39	4.49	4.62 (0.91)	4.48
A	4.89(5)	$^3E_1$, $\{\ldots 3a_1^2 1b_1^2 2e_1^3 3e_1^4 4a_1^1\}$	4.96	4.92	4.90 (0.89)	[g]
		$^3B_1$, $\{\ldots 3a_1^2 1b_1^1 2e_1^4 3e_1^4 4a_1^1\}$	5.42	5.37	5.46 (0.88)	5.29
		$^1E_1$, $\{\ldots 3a_1^2 1b_1^2 2e_1^3 3e_1^4 4a_1^1\}$	[f]	5.43	[g]	[g]
		$^1B_1$, $\{\ldots 3a_1^2 1b_1^1 2e_1^4 3e_1^4 4a_1^1\}$	[f]	5.59	[g]	[g]
B	5.98(3)	$^3A_1$, $\{\ldots 3a_1^1 1b_1^2 2e_1^4 3e_1^4 4a_1^1\}$	5.83	5.70	6.52 (0.81)	[g]

[a]Numbers in parentheses represent the uncertainty in the last digit.
[b]VDEs were calculated at TD-B3LYP/6–311+G(2*df*)//B3LYP/6–311+G*.
[c]VDEs were calculated at TD-PBE1PBE/6–311+G(2*df*)//B3LYP/6–311+G*.
[d]VDEs were calculated at UOVGF/6–311+G(2*df*)//B3LYP/6–311+G*. Values in parentheses represent the pole strength of the OVGF calculation.
[e]VDEs were calculated at UCCSD(T)/6–311+G(2*df*)//B3LYP/6–311+G*.
[f]We were not able to calculate these VDEs at the TD-B3LYP/6–311+G(2*df*)//B3LYP/6–311+G* level. (the calculations terminate with the "Fatal problem: The smallest alpha delta epsilon is –0.94992484D-02").
[g]VDE value cannot be calculated due to limitation of the theory.

TABLE II. Experimentally observed and theoretically calculated VDEs for the isomer II.1 (C_{7v}, $^1A_1$) of AlB_8^-. All energies are in eV.

Feature	VDE (expt.)[a]	Final state and electronic configuration	VDE (theo.) TD-B3LYP[b]	TD- PBE1PBE[c]	ROVGF[d]	UCCSD(T)[e]
X	3.66(5)	$^2A_1$, {…$3a_1^2 1e_3^4 2e_1^4 3e_1^4 4a_1^1$}	3.78	3.71	3.80 (0.89)	3.70
A	4.07(4)	$^2E_1$, {…$3a_1^2 1e_3^4 2e_1^4 3e_1^3 4a_1^2$}	3.73	3.93	4.02 (0.88)	4.05
B	5.12(5)	$^2E_1$, {…$3a_1^2 1e_3^4 2e_1^3 3e_1^4 4a_1^2$}	4.78	5.02	4.97 (0.89)	[f]
		$^2E_3$, {…$3a_1^2 1e_3^3 2e_1^4 3e_1^4 4a_1^2$}	6.18	6.41	6.65 (0.87)	[f]

[a]Numbers in parentheses represent the uncertainty in the last digit.
[b]VDEs were calculated at TD-B3LYP/6–311+G(2*df*)//B3LYP/6–311+G*.
[c]VDEs were calculated at TD-PBE1PBE/6–311+G(2*df*)//B3LYP/6–311+G*.
[d]VDEs were calculated at ROVGF/6–311+G(2*df*)//B3LYP/6–311+G*. Values in parentheses represent the pole strength of the OVGF calculation.
[e]VDEs were calculated at UCCSD(T)/6–311+G(2*df*)//B3LYP/6–311+G*.
[f]VDE value cannot be calculated due to limitation of the theory.

B. AlB_8^-

The 266 nm spectrum of AlB_8^- displays two well-resolved detachment bands (Fig. 2(a)). The X band with a VDE of 3.66 ± 0.05 eV is again very broad with a long tail on the lower binding energy side, suggesting a large geometry change from the ground state of AlB_8^- to that of the corresponding AlB_8 neutral structure. A detachment threshold is estimated to be ~3.1 eV. The A band with a VDE of 4.07 ± 0.04 eV is relatively sharp, but it seems to contain a shoulder on the higher binding energy side. In the 193 nm spectrum (Fig. 2(b)), a higher binding energy band (B) with a VDE of 5.12 ± 0.05 eV is observed. No other spectral transitions are observed beyond 5.5 eV in the 193 nm spectrum.

V. THEORETICAL RESULTS

A. AlB_7^-

The initial CK search for the global minimum of AlB_7^- was performed at the B3LYP/3–21G level of theory. The low-lying isomers revealed by the search (ΔE < 20 kcal/mol) are presented in Fig. 3. The geometries of all the low-lying isomers I.1 to I.5 were reoptimized with follow up frequency calculations at the B3LYP/6–311+G* level of theory. Single point calculations were performed at the RCCSD(T)/6–311+G(2*df*) level at the B3LYP/6–311+G* optimized geometries. At the B3LYP/6–311+G* level the structures I.2 and I.3 were found to be only 2.0 and 2.4 kcal/mol higher in energy than the global minimum isomer I.1 (C_{6v}, $^2A_1$). However, the structure I.2 is a first order saddle point with an imaginary frequency of 70 cm^{-1}. Geometry optimization following the imaginary frequency mode led to a slightly non-planar structure, which is only 0.01 kcal/mol lower in energy than the structure I.2. With zero-point energy (ZPE) correction the planar structure is actually 0.1 kcal/mol lower in energy. Thus, the planar structure I.2 (C_{2v}, $^2B_1$) should be considered as the second-lowest isomer. According to our highest level of theory, RCCSD(T)/6–311+G(2*df*), the relative energies of the I.2 and I.3 structures are 13.6 and 20.9 kcal/mol, respectively. Thus, only isomer I.1 is expected to be present in the cluster beam.

The valence isoelectronic B_8^- cluster was shown previously to possess a slightly distorted heptagonal wheel-type planar global minimum structure (C_{2v}, $^2B_1$),[2] which can be compared with the isomer I.2 of AlB_7^-. The umbrella-type isomer for B_8^- (D_{6h}, $^2A_{1g}$), similar to the structure I.1 of AlB_7^- cluster, was found to be 25.0 kcal/mol (B3LYP/6–311+G*) higher in energy than the global minimum planar structure of B_8^-. Clearly, the substitution of one B atom by an Al atom led to an inversion of the relative stabilities of the wheel-type versus the umbrella-type structures between B_8^- and AlB_7^-.

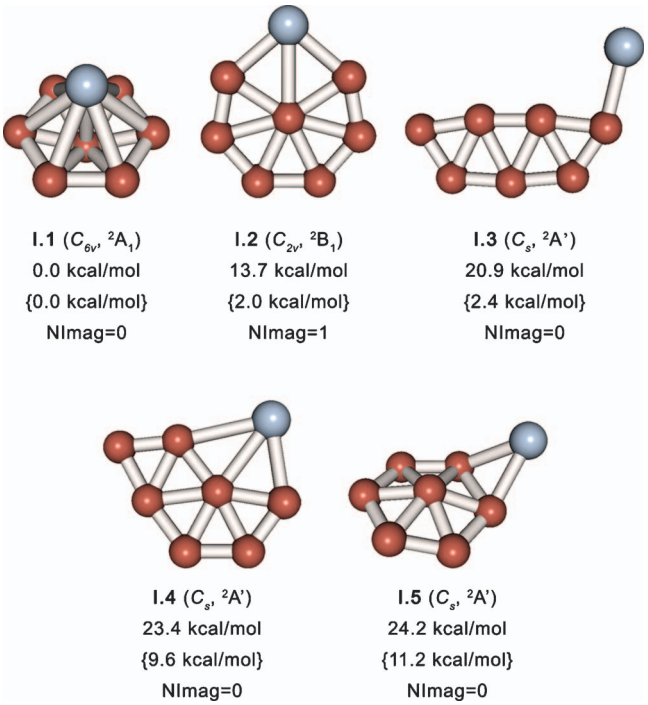

FIG. 3. Optimized structures of the AlB_7^- cluster, their point group symmetries, spectroscopic states, and relative energies. Relative energies are given at the RCCSD(T)/6–311+G(2*df*)//B3LYP/6–311+G* and the B3LYP/6–311+G* (in squiggle brackets) levels of theory. All the relative energies are ZPE corrected. NImag is the number of imaginary frequencies at B3LYP/6–311+G*.

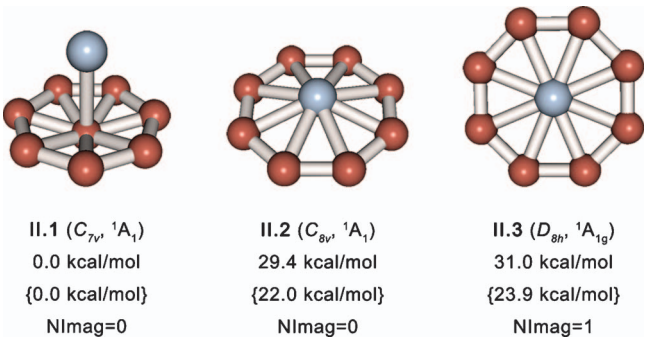

FIG. 4. Optimized structures of the AlB_8^- cluster, their point group symmetries, spectroscopic states, and relative energies. Relative energies are given at the RCCSD(T)/6–311+G(2*df*)//B3LYP/6–311+G* and the B3LYP/6–311+G* (in squiggle brackets) levels of theory. All the relative energies are ZPE corrected. NImag is the number of imaginary frequencies at B3LYP/6–311+G*.

B. AlB_8^-

The CK search for the global minimum structure of AlB_8^- at the B3LYP/3–21G level of theory revealed only three structures with relative energies $\Delta E < 30$ kcal/mol. The structures were reoptimized at the B3LYP/6–311+G* level of theory and single point RCCSD(T) calculations were performed on these geometries. The results are summarized in Fig. 4. The highly symmetrical planar structure II.3 (D_{8h}, $^1A_{1g}$) with the octacoordinated Al atom is 31.0 kcal/mol (RCCSD(T)/6–311+G(2*df*)//B3LYP/6–311+G*) higher in energy than the global minimum structure II.1 (C_{7v}, $^1A_1$). Moreover, this structure is a first order saddle point. Geometry optimization following the imaginary frequency mode led to the structure II.2 with the Al atom being 0.53 Å above the plane. Thus, the B_8 ring is clearly too small to host an Al atom in the center. The barrier for planarization is only 1.6 kcal/mol (RCCSD(T)/6–311+G(2*df*)//B3LYP/6–311+G*). The second lowest isomer II.2 (C_{8v}, $^1A_1$) is 29.4 kcal/mol higher in energy at RCCSD(T)/6–311+G(2*df*)//B3LYP/6–311+G* level than the global minimum isomer II.1. Thus, only isomer II.1 is expected to be present in the cluster beam.

The global minimum of the valence isoelectronic B_9^- cluster was shown previously to be a perfect molecular wheel (D_{8v}, $^1A_{1g}$).[1] The umbrella-type isomer (D_{7h}, $^1A_1'$), which is similar to the structure II.1 (C_{7v}, $^1A_1$) of the AlB_8^- cluster, is 31.1 kcal/mol (B3LYP/6—311 + G*) higher in energy than the global minimum planar structure of B_9^-. Moreover, this structure was found to be a second order saddle point. Geometry optimization following the imaginary frequency mode led to a distorted umbrella-type structure, which is 23.0 kcal/mol (B3LYP/6–311+G*) or 6.3 kcal/mol (RCCSD(T)/cc-pvTZ), Ref. 49 higher in energy than the global minimum. Again, the substitution of one B atom by an Al atom led to significant structural changes in the AlB_8^- cluster.

VI. INTERPRETATION OF THE PHOTOELECTRONIC SPECTRA

A. AlB_7^-

The calculated VDEs for the global minimum isomer I.1 are compared with the experimental data in Table I.

The first calculated VDE corresponds to the electron detachment channel from the HOMO-1 ($3e_1$) leading to the final triplet state $^3E_1$. Although the calculated VDE at B3LYP (3.02 eV) is somewhat lower than the experimental value, the calculated values at PBE1PBE (3.28 eV), UOVGF (3.30 eV), and UCCSD(T) (3.27 eV) are in excellent agreement with the experimental VDE of 3.3 eV. In this particular case, we found very little spin contamination in unrestricted Hartree-Fock UHF (also UOVGF and UCCSD(T)) for the ground doublet state and two triplet states, $^3E_1$ and $^3B_1$. The triplet nature of the final state of the first VDE is consistent with the high intensity of the experimental feature X. The second VDE corresponds to the transition into the $^1E_1$ final state with the electron detachment from HOMO-1 ($3e_1$). We were not able to calculate VDE for this transition at B3LYP but our VDE of 3.42 eV at PBE1PBE could be responsible for the weak shoulder in the 266 nm spectrum. The next transition into the final singlet state according to our calculations corresponds to the electron detachment from HOMO ($4a_1$) with calculated VDEs of 4.48 eV (UCCSD(T)), 4.62 eV (UOVGF), 4.39 eV (B3LYP), and 4.49 eV (PBE1PBE). However, there is no any prominent feature in this part of the experimental spectrum at 193 nm, though a small peak is present in the spectrum at 266 nm. Since transitions to final triplet states are much more prominent in the experimental spectra, we will further consider those transitions only. The next transition to the final triplet state with the electron detachment from HOMO-2 ($2e_1$) was calculated to be at 4.90 eV (UOVGF), 4.96 eV (B3LYP), and 4.92 eV (PBE1PBE). These numbers are in excellent agreement with the experimental feature A at 4.89 eV. According to our calculations, there is another transition from HOMO-3 ($3b_1$) into the final triplet state $^3B_1$ with the calculated VDEs 5.29 eV (UCCSD(T)), 5.46 eV (UOVGF), 5.42 eV (B3LYP), and 5.37 eV (PBE1PBE). There is no any prominent feature in this part of the spectrum, but the broad right shoulder of the feature A could be due to this transition. Finally, there is a prominent feature B in the experimental spectrum at 5.98 eV. According to our calculations that could be a transition to the final triplet state with the electron detachment from HOMO-4 ($3a_1$). Calculated VDEs at all levels of theory are way off from the experimental value, again because of the multi-configurational nature of the final state.

We optimized the neutral AlB_7 structure obtained by the detachment of an electron from the HOMO-1 ($3e_1$) of AlB_7^-, as shown in Fig. 5. We found that there is an appreciable geometry change from AlB_7^- (C_{2v}, $^2A_1$) to AlB_7 (C_{2v}, $^3B_1$). This structural relaxation is consistent with broad X band observed in the PES spectra. Overall, the theoretical results are in good agreement with the experimental data, confirming isomer I.1 as the global minimum for AlB_7^-.

B. AlB_8^-

The calculated VDEs from the global minimum of AlB_8^- are compared with the experimental data in Table II.

Since the AlB_8^- anion is a closed-shell system, one-electron detachments lead only to doublet final states. The first calculated VDE corresponds to electron detachment from

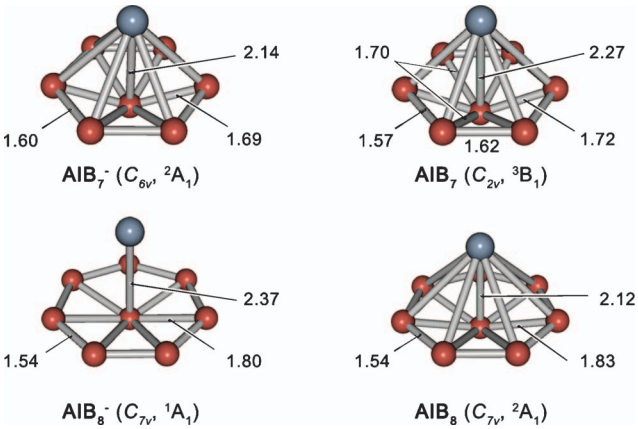

FIG. 5. Optimized structures (B3LYP/6–311+G*) of AlB_7^- (C_{6v}, $^2A_1$), AlB_8^- (C_{7v}, $^1A_1$), AlB_7 (C_{2v}, $^3B_1$), and AlB_8 (C_{7v}, $^2A_1$). Bond lengths are given in Å.

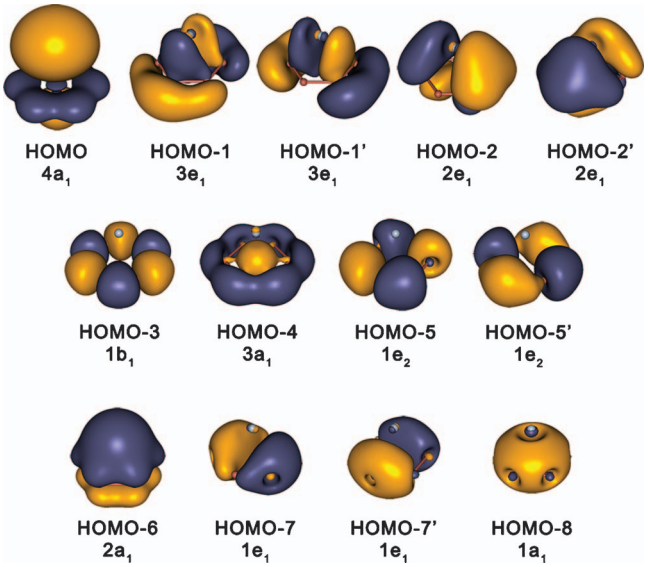

FIG. 6. Valence canonical molecular orbitals of the global minimum I.1 isomer of AlB_7^- (B3LYP/6–311+G*).

HOMO ($4a_1$). The theoretical values 3.70 eV (UCCSD(T)), 3.80 eV (UOVGF), 3.78 eV (B3LYP), and 3.71 (PBE1PBE) are all in excellent agreement with the experimental feature X at 3.66 eV. The second VDE can be assigned to an electron detachment from HOMO-1 ($3e_1$). The calculated values 3.93 eV (PBE1PBE), 4.05 eV (UCCSD(T)), and 4.02 eV (UOVGF) are congruous to the experimental feature A at 4.07 eV. Though, the calculated VDE at B3LYP (3.73 eV) is appreciably lower than the experimental value. The B band in the experimental spectrum (VDE = 5.12 eV) is assigned to photodetachment from HOMO-2 ($2e_1$) and the corresponding theoretical VDEs are 4.78 eV (B3LYP), 5.02 eV (PBE1PBE), and 4.97 (UOVGF). The photodetachment from HOMO-3 and HOMO-4 have VDE values that are too high in energy to be probed at 193 nm.

We also optimized the structure of the neutral C_{7v} AlB_8 upon removal of an electron from the HOMO of AlB_8^-, as shown in Fig. 5. We found a very large increase in the interaction between the Al atom and the B_8 fragment. The Al–B distances with the peripheral B atoms are reduced from 2.37 Å in the anion AlB_8^- (C_{7v}, $^1A_1$) to 2.12 Å in the neutral AlB_8 (C_{7v}, $^2A_1$) . Such a large structural change is consistent with the broad X band observed in the PES spectra of AlB_8^-. Overall, the theoretical results are in excellent agreement with the experimental observations, confirming unequivocally the umbrella-type structure II.1 as the global minimum for AlB_8^-.

VII. CHEMICAL BONDING

A. AlB_7^-

Chemical bonding in the global minimum structure I.1 of the AlB_7^- cluster can be formally described as the Al^{2+} cation coordinated to the B_7^{3-} anion in the ionic limit. NBO analysis of I.1 revealed that the effective atomic charges on aluminum and B_7 are +0.94|e| and −1.94|e|, respectively, which are significantly off from the ionic limit, though, this kind of deviation is expected. This charge distribution is consistent with the suggested bonding model for the AlB_7^- cluster. It was previously shown[50] that the B_7^- cluster has a pyramidal (C_{6v}, $^3A_2$) global minimum structure. Chemical bonding analysis[3,50] performed for the planar B_7^- (D_{6h}, $^3A_{2g}$) structure revealed six peripheral 2c–2e bonds, three delocalized σ B–B bonds with six σ-electrons responsible for its σ-aromaticity (the $4n + 2$ rule for singlet coupled electrons), and three delocalized π-bonds with four π-electrons responsible for its π-aromaticity (the $4n$ rule for triplet coupled electrons). Although the σ- and π-MOs in the pyramidal structure are mixed, the bonding picture developed for the planar structure is still believed to be qualitatively valid and can explain why the B_7^- cluster adopts the high symmetry C_{6v} structure.

Two extra electrons occupy the semi-occupied $3e_1$ orbital of B_7^- when we proceed to the B_7^{3-} anion making the orbital completely occupied and the cluster doubly aromatic with six delocalized σ-electrons and six delocalized π-electrons. Since formal charge on the aluminum atom is +2|e|, one electron is located primarily on the aluminum atom. This electron occupies the HOMO in AlB_7^-, and it was revealed by the NBO analysis that 95% of its density is located on the aluminum atom. Valence canonical molecular orbitals of the global minimum I.1 isomer of AlB_7^- are presented on Fig. 6. As it was shown before[3,50–52] the set of six MOs (HOMO-8, HOMO-7, HOMO-7′, HOMO-5, HOMO-5′, and HOMO-3) is responsible for the peripheral bonding and can be localized into six 2c–2e σ B–B bonds. HOMO-6, HOMO-2, and HOMO-2′ can be approximately assigned to delocalized π-bonds and thus, the system is formally "π-aromatic." HOMO-4, HOMO-1, and HOMO-1′ can be approximately assigned to delocalized σ-bonds and the system is formally "σ-aromatic." The singly-occupied HOMO being primarily the 3*s* AO of aluminum is consistent with NBO analysis results (Fig. 6).

B. AlB_8^-

Taking a similar approach to the one we used for AlB_7^- the global minimum II.1 of the AlB_8^- cluster can be

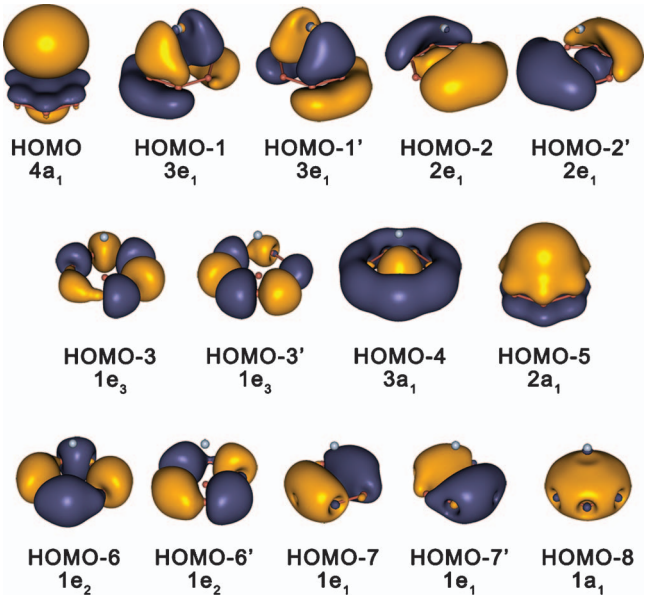

FIG. 7. Valence canonical molecular orbitals of the global minimum II.1 isomer of AlB_8^- (B3LYP/6–311 +G*).

considered as the Al^+ cation coordinated to the B_8^{2-} anion in the ionic limit. The model is consistent with the charge distribution revealed by the NBO analysis (+0.48|e| on aluminum and −1.48|e| on B_8), though, again the charges are expectedly lower than the ionic limit. The B_8^{2-} anion has a wheel-type (D_{7h}, $^1A_1'$) structure.[3,14] With the total of 26 valence electrons, 14 form seven 2c–2e peripheral σ B–B bonds, six electrons are responsible for the delocalized π-bonding and the six left are responsible for the delocalized σ-bonding. Thus, the B_8^{2-} anion is doubly (σ- and π-) aromatic. As it was shown in a joint experimental and theoretical study,[14] the LiB_8^- anion has a "half-sandwich" structure with the Li^+ cation bound to the almost unperturbed B_8^{2-} dianion. We have a similar bonding pattern for the AlB_8^- cluster with about the same perturbation from Al^+ cation on the B_8^{2-} dianion (the central boron atom is pushed out plane of the boron cycle by 0.32 Å compared to the 0.29 Å in LiB_8^-).

Valence canonical molecular orbitals of the global minimum II.1 isomer of AlB_8^- are presented in Fig. 7.

As it was shown before[2,3] the set of seven MOs (HOMO-8, HOMO-7, HOMO-7′, HOMO-6, HOMO-6′, HOMO-3, and HOMO-3′) form the peripheral bonding and can be localized into seven 2c–2e σ B–B bonds. HOMO-5 and HOMO-1 and HOMO-1′ can be approximately assigned to delocalized π-bonds and thus, the system is formally "π-aromatic." HOMO-4, HOMO-2 and HOMO-2′ can be approximately assigned to delocalized σ-bonds and thus, the system is formally "σ-aromatic." The doubly-occupied HOMO is primarily the 3*s* AO of aluminum as one can see from Fig. 7.

With this chemical model for two umbrella-type isomers I.1 (AlB_7^-) and II.1 (AlB_8^-), we can explain why the distance between aluminum and the central boron atom is shorter in AlB_7^- than in AlB_8^- (2.14 and 2.37 Å, respectively). Indeed, since the formal charge of aluminum is +2|e| and that of B_7 is –3|e| compared to the formal charge of aluminum +1|e| and that of B_8 –2|e|, one would expect a stronger bonding between aluminum atom and boron fragment in the first case. Though, the multiply charged B_7^{3-} and B_8^{2-} are not electronically stable in the isolated state the overall stability is achieved in AlB_7^- and AlB_8^- due to the external field of Al^{2+} and Al^+ cations, respectively. Our chemical bonding model can also explain why, upon electron detachment, the Al-B bond gets longer in AlB_7^- and shortens in AlB_8^-. In AlB_7^- the extra electron goes from the B_7^{3-} anion making the charge distribution Al^{2+} and B_7^{2-}, while in AlB_8^- the extra electron leaves the Al atom leading to the charge distribution Al^{2+} and B_8^{2-}.

VIII. SUMMARY

We investigated the AlB_7^- and AlB_8^- clusters in a combined photoelectron spectroscopy and *ab initio* study and established the global minimum umbrella-type structures for these clusters. Chemical bonding in the umbrella-type structure of the AlB_7^- cluster can be viewed as an Al^{2+} cation coordinated to a B_7^{3-} anion and the AlB_8^- cluster can be described as an Al^+ cation coordinated to a B_8^{2-} anion. The B_7^{3-} anion in the AlB_7^- cluster has six peripheral 2c–2e σ-bonds, three delocalized π-bonds responsible for the formal "π-aromaticity" and three delocalized σ-bonds (formal "σ-aromaticity"). Similarly, the B_8^{2-} anion in the AlB_8^- cluster is formally "σ- and π-aromatic" with seven peripheral 2c–2e σ–bonds, three delocalized π-bonds, and three delocalized σ-bonds. Apparently, the high stability of the umbrella type structures is due to the high stabilities of the quasiplanar B_7^{3-} and B_8^{2-} fragments derived from their doubly aromatic nature. The current study provides additional evidence for the robustness of the molecular wheel boron clusters and the importance of aromaticity in their stability. T.R.G. wishes to thank Utah State University for the Vice President for Research Graduate Fellowship.

ACKNOWLEDGMENTS

We thank Dr. Hua-Jin Zhai for help in the early part of the experiment. This research was supported by the National Science Foundation (NSF) (DMR-0904034 to L.S.W. and CHE-1057746 to A.I.B.). An allocation of computer time from the Center for High Performance Computing at the University of Utah is gratefully acknowledged. Computer time from the Center for High Performance Computing at Utah State University is also gratefully acknowledged. T.R.G. wishes to thank Utah State University for the Vice President for Research Graduate Fellowship.

[1] H. J. Zhai, A. N. Alexandrova, K. A. Birch, A. I. Boldyrev, and L. S. Wang, Angew. Chem. Int. Ed. **42**, 6004 (2003).
[2] A. N. Alexandrova, A. I. Boldyrev, H. J. Zhai, and L. S. Wang, Coord. Chem. Rev. **250**, 2811 (2006).
[3] D. Y. Zubarev and A. I. Boldyrev, J. Comput. Chem. **28**, 251 (2007).
[4] H. J. Zhai, L. S. Wang, D. Y. Zubarev, and A. I. Boldyrev, J. Phys. Chem. A **110**, 1689 (2006).
[5] H. J. Zhai, C. Q. Miao, S. D. Li, and L. S. Wang, J. Phys. Chem. A **114**, 12155 (2010).
[6] B. Kiran, X. Li, H. J. Zhai, L. F. Cui, and L. S. Wang, Angew. Chem. Int. Ed. **43**, 2125 (2004).
[7] Z. Y. Jiang, X. M. Luo, S. T. Li, and S. Y. Chu, Int. J. Mass Spectrom. **252**, 197 (2006).

[8]H. Kawamata, Y. Negishi, A. Nakajima, and K. Kaya, Chem. Phys. Lett. **337**, 255 (2001).
[9]B. B. Averkiev and A. I. Boldyrev, Russ. J. Gen. Chem. **78**, 769 (2008).
[10]B. B. Averkiev, L. M. Wang, W. Huang, L. S. Wang, and A. I. Boldyrev, Phys. Chem. Chem. Phys. **11**, 9840 (2009).
[11]X. J. Feng and Y. H. Luo, J. Phys. Chem. A **111**, 2420 (2007).
[12]J. C. Guo, W. Z. Yao, Z. Li, and S. D. Li, Sci. China Ser. B: Chem. **52**, 566 (2009).
[13]C. Romanescu, A. Sergeeva, W.-L. Li, A. I. Boldyrev, and L. S. Wang, J. Am. Chem. Soc. **113**, 8646 (2011).
[14]A. N. Alexandrova, H. J. Zhai, L. S. Wang, and A. I. Boldyrev, Inorg. Chem. **43**, 3552 (2004).
[15]J. Simons, J. Phys. Chem. A **112**, 6401 (2008).
[16]J. Simons, Annu. Rev. Phys. Chem. **62**, 107 (2011).
[17]L. S. Wang, H. S. Cheng, and J. W. Fan, J. Chem. Phys. **102**, 9480 (1995).
[18]L. S. Wang and H. Wu, in *Advances in Metal and Semiconductor Clusters*, edited by M. A. Duncan (JAI, Greenwich, CT, 1998), Vol. 4, pp. 299–343.
[19]J. Akola, M. Manninen, H. Hakkinen, U. Landman, X. Li, and L. S. Wang, Phys. Rev. B **60**, 11297 (1999).
[20]L. S. Wang and X. Li, in *Proceedings International Symposium on Clusters and Nanostructure Interfaces, Richmond, VA, 25–28 October 1999*, edited by P. Jena, S. N. Khanna, and B. K. Rao (World Scientific, River Edge, New Jersey, 2000), pp. 293–300.
[21]W. Huang and L. S. Wang, Phys. Rev. Lett. **102**, 153401 (2009).
[22]A. P. Sergeeva, B. B. Averkiev, H. J. Zhai, A. I. Boldyrev, and L. S. Wang, J. Chem. Phys. **134**, 224304 (2011)
[23]A. D. Becke, J. Chem. Phys. **98**, 5648 (1993).
[24]S. H. Vosko, L. Wilk, and M. Nusair, Can. J. Phys. **58**, 1200 (1980).
[25]C. T. Lee, W. T. Yang, and R. G. Parr, Phys. Rev. B **37**, 785 (1988).
[26]J. Binkley, J. A. Pople, and W. J. Hehre, J. Am. Chem. Soc. **102**, 939 (1980)
[27]M. S. Gordon, J. S. Binkley, J. A. Pople, W. J. Pietro, and W. J. Hehre, J. Am. Chem. Soc. **104**, 2797 (1982).
[28]A. D. McLean and G. S. Chandler, J. Chem. Phys. **72**, 5639 (1980).
[29]W. J. Pietro, M. M. Francl, W. J. Hehre, D. J. Defrees, J. A. Pople, and J. S. Binkley, J. Am. Chem. Soc. **104**, 5039 (1982).
[30]T. Clark, J. Chandrasekhar, G. W. Spitznagel, and P. v. R. Schleyer, J. Comput. Chem. **4**, 294 (1983).
[31]J. Cizek, Adv. Chem. Phys. **14**, 35 (1969).
[32]G. D. Purvis and R. J. Bartlett, J. Chem. Phys. **76**, 1910 (1982).
[33]K. Raghavachari, G. W. Trucks, J. A. Pople, and M. Head-Gordon, Chem. Phys. Lett. **157**, 479 (1989).
[34]L. S. Cederbaum, J. Phys. B **8**, 290 (1975).
[35]J. V. Ortiz, Int. J. Quantum Chem. **36**(S23), 321 (1989).
[36]J. S. Lin and J. V. Ortiz, Chem. Phys. Lett. **171**, 197 (1990).
[37]V. G. Zakrzewski, J. V. Ortiz, J. A. Nichols, D. Heryadi, D. L. Yeager, and J. T. Golab, Int. J. Quantum Chem. **60**, 29 (1996).
[38]R. Bauernschmitt and R. Ahlrichs, Chem. Phys. Lett. **256**, 454 (1996).
[39]M. E. Casida, C. Jamorski, K. C. Casida, and D. R. Salahub, J. Chem. Phys. **108**, 4439 (1998).
[40]J. P. Perdew, K. Burke, and M. Ernzerhof, Phys. Rev. Lett. **77**, 3865 (1996).
[41]J. P. Perdew, K. Burke, and M. Ernzerhof, Phys. Rev. Lett. **78**, 1396 (1997).
[42]J. P. Foster and F. Weinhold, J. Am. Chem. Soc. **102**, 7211 (1980).
[43]A. E. Reed, L. A. Curtiss, and F. Weinhold, Chem. Rev. **88**, 899 (1988).
[44]F. Weinhold and C. R. Landis, *Valency and Bonding: A Natural Bond Orbital Donor-Acceptor Perspective* (Cambridge University Press, Cambridge, England, 2005).
[45]M. J. Frisch, G. W. Trucks, and H. B. Schlegel *et al.*, Gaussian 03, revision D.01; Gaussian, Inc., Wallingford, CT, 2004.
[46]H.-J. Werner, P. J. Knowles, G. Knizia, F. R. Manby, M. Schütz *et al.*; MOLPRO, a package of *ab initio* programs, version 2006.1, see http://www.molpro.net.
[47]G. Schaftnenaar, molden3.4, CAOS/CAMM Center, The Netherlands (1998).
[48]U. Varetto, MOLEKEL 5.4.0.8, Swiss National Supercomputing Centre: Manno (Switzerland) (2009).
[49]L. L. Pan, J. Li, and L. S. Wang, J. Chem. Phys. **129**, 024302 (2008).
[50]A. N. Alexandrova, A. I. Boldyrev, H. J. Zhai, and L. S. Wang, J. Phys. Chem. A **108**, 3509 (2004).
[51]P. W. Fowler and B. R. Gray, Inorg. Chem. **46**, 2892 (2007).
[52]D. Y. Zubarev and A. I. Boldyrev, Phys. Chem. Chem. Phys. **10**, 5207 (2008).